Optical Properties and Electronic Structure of Amorphous Germanium

By

J. Tauc (a), R. Grigorovici (b), and A. Vancu (b)

The optical constants of amorphous Ge are determined for photon energies from 0.08 to 1.6 eV. From 0.08 to 0.5 eV, the absorption is due to k-conserving transitions of holes between the valence bands as in p-type crystals; the spin-orbit splitting is found to be 0.20 and 0.21 eV in non-annealed, and annealed samples respectively. The effective masses of the holes in the three bands are 0.49 m (respectively 0.43 m); 0.04 m, and 0.08 m. An absorption band is observed below the main absorption edge (at 300 °K the maximum of this band is at 0.86 eV); the absorption in this band increases with increasing temperature. This band is considered to be due to excitons bound to neutral acceptors, and these are presumably the same ones that play a decisive role in the transport properties and which are considered to be associated with vacancies. The absorption edge has the form: $\omega^2 \varepsilon_2 \sim (\hbar \omega - E_g)^2$ ($E_g = 0.88$ eV at 300 °K). This suggests that the optical transitions conserve energy but not k vector, and that the densities of states near the band extrema have the same energy-dependence as in crystalline Ge. A simple theory describing this situation is proposed, and comparison of it with the experimental results leads to an estimate of the localization of the conduction-band wavefunctions.

Für amorphes Germanium werden die optischen Konstanten für Photonenenergien von 0,08 bis 1,6 eV bestimmt. Zwischen 0,08 bis 0,5 eV wird die Absorption wie in p-leitenden Kristallen durch Übergänge von Löchern mit k-Erhaltung zwischen den Valenzbändern hervorgerufen. Die Spin–Bahn-Aufspaltung wird zu 0,20 bzw. 0,21 eV in nichtgetemperten bzw. getemperten Proben gefunden. Die effektiven Massen der Löcher in den drei Bändern sind 0,49 m (bzw. 0,43 m); 0,04 m und 0,08 m. Eine Absorptionsbande wird unterhalb der Hauptabsorptionskante beobachtet (bei 300 °K liegt das Maximum dieser Bande bei 0,86 eV). Die Absorption in dieser Bande wächst mit steigender Temperatur an. Es wird angenommen, daß diese Absorptionsbande durch an neutrale Akzeptoren gebundene Exzitonen hervorgerufen wird und daß diese Akzeptoren vermutlich die gleichen sind, die eine entscheidende Rolle bei den Transporteigenschaften spielen. Von diesen nimmt man an, daß sie mit Lücken verbunden sind. Die Absorptionskante ist von der Form: $\omega^2 \varepsilon_2 \sim (\hbar \omega - E_g)^2$ ($E_g = 0,88$ eV bei 300 °K). Dies weist darauf hin, daß die optischen Übergänge zwar die Energie, nicht aber den k-Vektor erhalten und daß die Zustandsdichte in der Nähe der Bandextrema die gleiche Energieabhängigkeit wie in kristallinem Germanium besitzt. Es wird eine einfache Theorie vorgeschlagen, die diese Situation beschreibt. Ein Vergleich dieser Theorie mit den experimentellen Ergebnissen ergibt eine Abschätzung für die Lokalisierung der Leitungsband-Wellenfunktionen.

1. Introduction

The optical constants of amorphous germanium were determined in the photon energy range 0.08 to 1.6 eV with the aim to obtain information about its electronic structure, in particular, about the differences between the crystalline and amorphous states. Germanium was chosen for this study because the electronic structure of the crystal is well known and because it is a relatively simple example of amorphous solid. One can hope that the basic features found

40*

in this simple case may be of interest for the interpretation of more complicated amorphous materials.

Another simple amorphous semiconductor is selenium; its optical properties and electronic structure have been extensively studied (cf. [1] and the references to older work quoted in this paper). The difficulty with selenium is that even in the crystalline state its band structure and transport properties are much less understood than those of germanium. Anyway, the crystalline structure of selenium is very different from that of germanium and although some features of amorphous Se and Ge are similar, one should not be surprised if there are also some differences.

Following the results of X-ray investigations of the structure (cf. [2]), we can imagine that in amorphous germanium the tetrahedra are the basic units as in the crystal, however, the neighbouring tetrahedra are irregularly rotated along the line joining two atoms. Neglecting small deformations of the tetrahedra, we have here an example of a solid with the same short range order as in the crystal, but without the long range order.

Similarly as in glasses (cf.e.g. [3]) the X-ray investigations are unable to decide between the two following possibilities: The layers of amorphous Ge may be composed of small crystallites (with linear dimensions of the order of magnitude 10 Å) or they may be considered as a homogeneous medium with the atomic pattern varying so that no long range order is detectable beyond say 20 Å. For the interpretation of the experimental results we use the "homogeneous" model. It seems, however, that the other model may be equally suitable. Should some observable difference be found, it may be possible to decide between both models. In the present paper this point is not discussed.

Another important feature of the structure of amorphous Ge is the necessary presence of vacancies as the irregularly rotated tetrahedra cannot completely fill the space. These vacancies may contain some foreign atoms; about this

here are serious difficulties with
and some other amorphous semi-
repared only in thin layers. This
s difficult in some regions of the
er large concentration of holes [4];
e presence of vacancies which act
y expect a large influence of the
determined on sufficiently thick
ere found to be the same and we
optical constants are those of the

vere published in [6]. The measure-
t conditions (cf. Section 2) and

Samples

on of very pure germanium from
and 10^{-6} Torr on a substrate kept
ion $\lambda > 2 \, \mu m$ potassium chloride
uartz substrates were used. The
ffraction and electron microscope.

From the experimental point of view tl
amorphous germanium as compared with Se
conductors because amorphous Ge can be p
makes the determination of optical constant
spectrum. These layers always contain a rath
their presence is probably connected with tl
as acceptors. As the layers are thin, one m
surface [5]. However, the optical constants
layers (thickness between 400 and 4000 Å w
consider this to be an indication that the c
"bulk" amorphous material.

Preliminary results of these investigations v
ments were partly repeated under differen
extended farther into the infrared region.

2. Preparation of

The samples were prepared by evaporati
tungsten crucibles in a vacuum between 10^{-5}
at room temperature. For the spectral reg
and for the rest of the spectrum fused qu
structure of the layers was tested by X-ray di

The optical measurements were usually performed on layers taken out of the evaporation apparatus and measured in air. Some measurements (at the absorption edge) were done in vacuum without taking the sample out of the evacuated space. No essential differences have been observed.

No special efforts have been made to deposit the layers in a vacuum better than 10^{-6} Torr because the measurement of electrical conductivity performed by Suhrmann et al. [7] in an ultra-high vacuum led to the same results as those performed in a vacuum between 10^{-5} and 10^{-6} Torr.

Another important fact is the possibility of converting the amorphous layers into polycrystalline layers by annealing them at a temperature between 400 and 450 °C. These polycrystalline layers have essentially the same properties as single crystals provided proper account is taken of the scattering of light on the surface irregularities of polycrystalline layers as briefly discussed in [6].

The amorphous layers could be annealed by keeping them at about 250 °C for several hours. As discussed in [4] after this process the layers are in an amorphous state, but the concentration of vacancies is decreased and the long range order increased. The measurements of optical properties were performed on amorphous non-annealed Ge (a-Ge) and amorphous annealed Ge $(a_t$-Ge), and some differences were found.

The thickness of the layers was determined from Tolansky fringes observed in an interference microscope. The results to be discussed later were obtained on the following layers:

a) For $\lambda > 2$ μm: two non-annealed samples (thicknesses 0.300 and 0.313 μm) and two samples (thicknesses 0.238 and 0.245 μm) measured before and after annealing.

b) For the main absorption edge region: five non-annealed samples (thicknesses 0.0785, 0.1113, 0.210, 0.253, and 0.466 μm) measured at room temperature. Three of them were measured also at 150 °K in vacuum, two samples annealed at 373 °K, and two samples annealed at 473 °K.

3. Experimental Method

The optical constants were determined by the measurement of transmission and reflection. For $\lambda > 2$ μm the double-beam Zeiss infrared monochromator UR 10 was used with an adaptor for the measurement of reflectivity designed by Vaško [8]. For shorter wavelengths Leiss double prism monochromator or Zeiss single prism monochromator SPM 1 were used. For the measurement of reflectivity either Abráham's [9] or Lukeš' [10] arrangement modified for convergent beams (convergence about 6°) were used, the latter for measurements at low temperatures in vacuum. PbS photocell (Mullard 61 SV), photo-multipliers (RCA 7102, EMI 62 56 B) and thermocouple (Zeiss VTh 1) were used as detectors in various spectral regions.

For the evaluation of the optical constants from the measured transmission and reflection the formulae quoted in Mayer's book [11] were applied. They take into account the interference effects both in the sample and in the substrate. The latter being always thick in our experiments, the corresponding interference terms have been averaged after Koller [12]. To facilitate the calculations we took a constant value for the refractive index of the substrates 1.45 for fused quartz and 1.52 for KCl.

We shall now discuss consecutively the various parts of the spectrum starting with lowest photon energies.

4. Transitions in the Valence Band

In Fig. 1 the imaginary part of the dielectric constant $\varepsilon_2 = 2\,n\,k$ is plotted against photon energy (for the real part of the refractive index cf. [6]) in the photon energy region below 0.6 eV. It is seen that the spectra observed on a-Ge or a_t-Ge show qualitatively a surprising similarity with the spectra observed in this region on crystalline p-type Ge [13 to 16]. At room temperature one observes in crystalline Ge two absorption peaks at 0.36 and 0.26 eV and an absorption edge at about 0.2 eV. In amorphous Ge one sees a similar structure, shifted however towards lower energies. The respective peaks are now at 0.28 and 0.165 eV in a-Ge and at 0.28 and 0.177 eV in a_t-Ge. The absorption edge lies at about 0.1 eV in both cases. The spectrum observed on the annealed sample is sharper than on the non-annealed sample, the difference being very striking for the peak near 0.17 eV.

In crystalline Ge these spectra have been interpreted as direct (i.e. k vector conserving) transitions of holes from the two upper valence bands 1 and 2 into the deep lying valence band 3 and between the two valence bands 1 and 2 (Fig. 2). For $k = 0$ the transitions are forbidden. The shape of the spectrum can be approximately described by the relations (cf. [16])

$$
\left.
\begin{aligned}
\omega^2\,\varepsilon_2^{13} &\sim |\hbar\,\omega - \Delta E|^{3/2} \exp\left[\frac{m_3}{m_3 - m_1}\,\frac{\hbar\,\omega - \Delta E}{k\,T}\right], \\[2mm]
\omega^2\,\varepsilon_2^{23} &\sim |\hbar\,\omega - \Delta E|^{3/2} \exp\left[\frac{m_3}{m_3 - m_2}\,\frac{\hbar\,\omega - \Delta E}{k\,T}\right], \\[2mm]
\omega^2\,\varepsilon_2^{12} &\sim (\hbar\,\omega)^{3/2}\left(\exp\left[\frac{m_2}{m_2 - m_1}\,\frac{\hbar\,\omega}{k\,T}\right] - \exp\left[\frac{m_1}{m_2 - m_1}\,\frac{\hbar\,\omega}{k\,T}\right]\right), \\[2mm]
\frac{1}{m_3} &\approx \frac{1}{2}\left(\frac{1}{m_1} + \frac{1}{m_2}\right).
\end{aligned}
\right\}
\tag{1}
$$

ε_2^{ij} is the imaginary part of the dielectric constant for the transitions of holes between the bands i and j, m_i the (average) effective mass of the band i. ΔE ist the energy difference caused by spin-orbit splitting between the top of the degenerate bands 1 and 2 and the top of the band 3 (Fig. 2). As the bands 1 and 2 are not parabolic, the third of equations (1) cannot be applied if the measurements
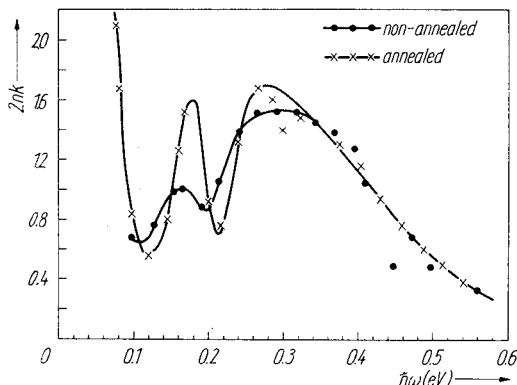

Fig. 1. Valence band transitions. The points are experimental results, the curves were calculated after equation (1)
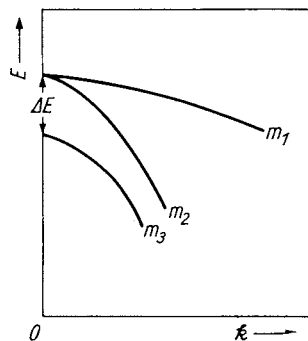
Fig. 2. Structure of the valence band of Ge

are not pushed far enough into the infrared [17]. The effective masses in crystalline Ge are $m_1 = 0.3\ m$, $m_2 = 0.04\ m$, and $m_3 = 0.08\ m$.

In amorphous Ge we find that the absorption bands are well described by formulae (1) (with the exception of the third one) with $\Delta E = 0.20$ eV for the non-annealed and $\Delta E = 0.21$ eV for the annealed samples. The effective masses are $m_1 = 0.49\ m$, $m_2 = 0.04\ m$ in non-annealed samples and $m_1 = 0.43\ m$, $m_2 = 0.04\ m$ in annealed samples, m_3 being assumed to be $0.08\ m$, as in crystalline Ge. This suggests that this part of the spectrum is of the same origin in amorphous Ge as in crystalline Ge.

Such a conclusion implies important consequences for the structure of the valence band near $k = 0$ in amorphous Ge. The structure of the valence band is qualitatively the same as in crystalline Ge. In particular, the top of the valence band is again doubly degenerate as in crystalline Ge and there exists a split-off valence band. The chief difference between both cases is the larger value of the heavy hole mass $m_1 = 0.49\ m$ (respectively $0.43\ m$) as compared with $0.3\ m$ in crystalline Ge and the smaller value of the spin-orbit splitting ΔE (0.20, respectively 0.21 eV as compared with 0.29 eV in crystalline Ge). It is remarkable that the value of the spin-orbit splitting in amorphous Ge lies between the value in the atom (0.18 eV) and that in the crystal and increases with annealing, i.e. by improving the degree of order.

It also appears that the k vector is well conserved during the transitions in this part of the spectrum. This holds in particular for annealed amorphous samples as the spectra are well described by formulae (1) based on direct transitions.

The value of the absorption constant must be proportional to the concentration of holes. If we compare the absorption coefficient with the absorption coefficient of highly doped crystalline Ge (after [15]) and assume that the matrix elements are roughly the same, we find the order of magnitude of the concentration of holes in amorphous Ge to be 10^{19} cm^{-3}. The strength of absorption measured by $\int \hbar\,\omega\,\varepsilon_2\,\mathrm{d}(\hbar\,\omega)$ decreases only slightly by annealing (by 14%). If the suggested explanation of the bands is correct, this implies that the concentration of holes at the top of the valence band changes only slightly during annealing.

It appears difficult to reconcile such a conclusion with the results of the measurement of electrical conductivity and barrier capacitance of junctions with a- or a_t-Ge; a large difference has been found [4]. This point is not understood presently.

Let us remark that a spectrum of a similar kind has been observed in amorphous Se. Kessler and Sutter [18] have shown by a conclusive experiment that it is indeed due to the transitions of holes between various branches of the valence band.

5. Tail of the Absorption Edge

In this section we shall consider the tail observed at the low energy side of the actual absorption edge (Figs. 3 and 4). This tail is an absorption band the shape of which can be found if proper extrapolation is applied to the absorption edge as discussed in the next section. It is seen that it has Gaussian shape. It is not a transition from or into the valence or conduction bands; one would expect in such cases the appearance of an edge rather than of a band.
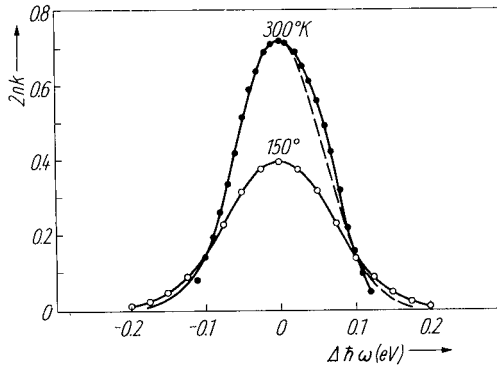
Fig. 3. Tail at the absorption edge at 300 and 150 °K. The dotted line is a Gaussian curve

The energy of transition is somewhat smaller than the activation energy of intrinsic conductivity and different from other activation energies observed in the conductivity vs. temperature curves. By these considerations we are led to ascribe the tail to a transition connected with a localized defect.

The band does not exist in crystalline Ge and its strength appears to be structure sensitive in amorphous Ge, being different in different samples. Very interesting is its temperature dependence. We see in Fig. 3 that the half-width of the band is approximately the same at 150 and 300 °K, but the integrated absorption measured by $\int \hbar \omega \, \varepsilon_2 \, d(\hbar \omega)$ is larger at the higher temperature by 45%.

We suggest that the tail is caused by excitons bound to acceptors. It is known from transport properties that amorphous germanium layers contain a large concentration of acceptors. It is believed that the vacancies necessarily present in such layers may act as acceptors (cf. [19]). We imagine that the following process takes place: An acceptor captures an electron by thermal excitation and the photon excites this electron into a state in which the acceptor binds an electron and a hole. Such a process should be proportional to the product of the concentration of ionized acceptors n_A and the concentration of holes p.

Let us consider the simplest possibility. In the material there are N_A acceptors/cm³ with an activation energy E_A und N_D donors/cm³ with energy levels many $k\,T$ above the energy level of acceptors; one has then $n_A = N_D + p$. In such a case the de Boer-van Geel formula gives

$$p\,n_A = (N_A - n_A)\,\frac{N_v}{\beta}\exp\left[-\frac{E_A}{k\,T}\right], \qquad (2)$$

where N_v is the effective density of states in the valence band, β the spin degeneracy of acceptors. In the case that $n_A/N_A \ll 1$ (or $p \ll N_A - N_D$) we obtain from the above given ratio 1.45 of integrated absorptions at 300 and 150 °K, $E_A = 0.01$ eV. Of course, we have no evidence that only a small part of acceptors is ionized and it may well be that the compensation is high and n_A/N_A may not be negligible compared with unity; in such a case we obtain for E_A a larger value than 0.01 eV. Detailed measurements of temperature dependence of the tail are necessary to obtain a definite information about the parameters of the statistics.

The maximum of the band lies in a-Ge at room temperature about 0.02 eV below the optical gap obtained by extrapolation of the absorption edge (as-

suming $\omega^2 \varepsilon_2 \sim (\hbar \omega - E_g)^2$ cf. Section 6). This energy difference is smaller in annealed samples and becomes even negative, the maximum lying inside the extrapolated band-to-band transitions. This may point to the fact that the extrapolation used is not precisely correct inside the tail.

The maximum of the peak shifts towards higher energies when the temperature is lowered ($\Delta E_{max}/\Delta T \approx - 1 \times 10^{-4}$ eV/deg).

The suggested explanation of this tail as caused by excitons bound to defects is in principle similar to the explanations of similar tails observed near the fundamental absorption edges of ionic crystals (α and β bands [20]).

The small difference between the optical gap and the tail band maximum energy seems to exclude another possibility for explaining the tail, that is as a transition of an electron from the ionized acceptor to a donor state (e.g. from a vacancy to the neighbouring interstitial atom). One would expect a lower energy for such a process as the donor states are unlikely to lie very close to the band edge.

6. Absorption Edge

In Fig. 4 $\hbar \omega \sqrt{\varepsilon_2}$ is plotted against $\hbar \omega$ near the absorption edge for one of the a-Ge samples. It is apparent that the absorption in the tail is followed by an absorption which is represented by a straight line showing that in this region $\omega^2 \varepsilon_2 \approx (\hbar \omega - E_g)^2$. If we extrapolate this line, we obtain at 300 °K in a-Ge $E_g = 0.88$ eV, in a_t-Ge $E_g = 0.92$ eV.

The dependence of ε_2 on $\hbar \omega$ near the absorption edge suggests that one has here transitions for which only energy but not the k vector is conserved (indirect transitions) as we suggested previously [6]. We shall sketch a brief reasoning which shows how this can be understood and what information is obtained from the observed shape of the absorption edge.

If the short range order is the same in amorphous and crystalline states we can consider the atomic arrangement in an amorphous solid as a perturbed lattice of the corresponding crystal. This point of view has been used in previous theoretical work (for a review cf. [21, 22]).

The wave functions in the valence and conduction bands of the crystal are Bloch functions:

$$|v \, \boldsymbol{k}\rangle = V^{-1/2} \, u_{v \boldsymbol{k}}(\boldsymbol{r}) \, e^{i \boldsymbol{k} \boldsymbol{r}}, \qquad |c \, \boldsymbol{k}'\rangle = V^{-1/2} \, u_{c \boldsymbol{k}'}(\boldsymbol{r}) \, e^{i \boldsymbol{k}' \boldsymbol{r}} \qquad (3)$$

normalized in the basic volume V; $\boldsymbol{k}, \boldsymbol{k}'$ are in the first Brillouin zone.
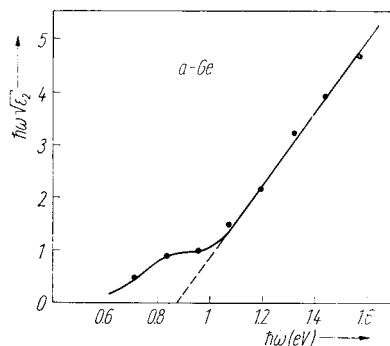

Fig. 4. Absorption edge of amorphous Ge at 300 °K

We shall make the following assumptions:

We assume that the basic volume V contains the same number of atoms in the amorphous as in the crystalline state (for simplicity we neglect the difference of densities of both states).

It is known both from experiment and theory that the valence and conduction bands retain their meaning in the amorphous state. We shall assume that the perturbation describing the change of the crystalline into the amorphous state is such that the wave functions in the valence band of the amorphous state are in zero approximation linear combinations of the wavefunctions in the valence band of the crystal; an analogous statement holds for the conduction band. Therefore, the ground state described by a Slater determinant is the same as in the crystal. If we now produce an electron hole pair in the crystal with wave functions $|v \varkappa\rangle$, $|c \varkappa'\rangle$ and then switch on the perturbation we obtain the wave functions in the amorphous solid. We can label these wave functions with indices $\varkappa$, $\varkappa'$ and denote them by $|v \varkappa\rangle_a$, $|c \varkappa'\rangle_a$. As the perturbation is performed in a continuous spectrum we can assume that the energies of the states $|v \varkappa\rangle_a$ and $|v \varkappa\rangle$ measured from the top of the valence band are the same (similarly for the conduction band). The consequence of these assumptions is that the corresponding densities of states are the same in both cases.

This approach has been suggested by Velický [23] and we shall show that it gives a good description of the observed shape of the absorption edge. We start from the general one-electron formula

$$\varepsilon_2(\omega) = \left(\frac{2 \pi e}{m \omega}\right)^2 \frac{1}{V} \sum_{i,f} |\boldsymbol{P}_{if}|^2 \, \delta \, (E_f - E_i - \hbar \, \omega) \,, \tag{4}$$

where the summation is performed over all initial and final states i, f in the basic volume V. $\boldsymbol{P}_{if}$ is the momentum matrix element between the wave functions of the final and initial states $|c \varkappa'\rangle_a$ and $|v \varkappa\rangle_a$. Expressing them as linear combinations of Bloch functions in the respective bands, we obtain

$$P_{if} = {}_a\langle c \varkappa'| \, \boldsymbol{p} \, |v \varkappa\rangle_a = \sum_{\boldsymbol{k}} \sum_{\boldsymbol{k}'} {}_a\langle c \varkappa'| \, c \, \boldsymbol{k}\rangle \, \langle v \, \boldsymbol{k}|v \varkappa\rangle_a \, \langle c \, \boldsymbol{k}'| \, \boldsymbol{p} \, |v \, \boldsymbol{k}\rangle =$$
$$= \sum_{\boldsymbol{k}} {}_a\langle c \varkappa'|c \, \boldsymbol{k}\rangle \, \langle v \, \boldsymbol{k}|v \varkappa\rangle_a \, \boldsymbol{p}_{vc}(\boldsymbol{k}) \,, \tag{5}$$

where

$$\boldsymbol{p}_{vc}(\boldsymbol{k}) = - i \, \hbar \, \frac{1}{\Omega} \int_{\text{cell}} \mathrm{d}^3 \boldsymbol{r} \, u_{v\boldsymbol{k}}^*(\boldsymbol{r}) \, \text{grad} \, u_{c\boldsymbol{k}}(\boldsymbol{r}) \tag{6}$$

is the matrix element in the crystal. The summations are performed over all $\boldsymbol{k}$ vectors in the first Brillouin zone. Ω is the volume of the elementary cell over which the integration is performed.

From (4) we obtain

$$\varepsilon_2(\omega) = \left(\frac{2 \pi e}{m \omega}\right)^2 \frac{2}{V} \sum_{\varkappa} \sum_{\varkappa'} \left| \sum_{\boldsymbol{k}} \boldsymbol{p}_{vc}(\boldsymbol{k}) \, {}_a\langle c \varkappa'|c \, \boldsymbol{k}\rangle \, \langle v \, \boldsymbol{k}|v \varkappa\rangle_a \right|^2 \times$$
$$\times \, \delta \, (E_c(\varkappa') - E_v(\varkappa) - \hbar \, \omega) \,. \tag{7}$$

The summations are over all $\varkappa$, $\varkappa'$ in the first Brillouin zone. The factor 2 takes care of the doubling of the number of states by spin which is conserved during the transition.

In the crystal we have

$$\langle c \varkappa'|c \, \boldsymbol{k}\rangle = \delta_{\boldsymbol{k}\varkappa'} \,, \qquad \langle v \, \boldsymbol{k}|v \varkappa\rangle = \delta_{\boldsymbol{k}\varkappa} \,.$$

Summing over k and $\varkappa'$ and replacing then $\sum\limits_{\varkappa}$ by $V/(2\pi)^3 \cdot \int\limits_B d^3\varkappa$ we obtain the usual formula for direct transitions:

$$\varepsilon_2(\omega) = \left(\frac{2\pi e}{m\omega}\right)^2 \frac{2}{(2\pi)^3} \int\limits_B d^3\varkappa\, |\boldsymbol{p}_{v\,c}(\varkappa)|^2\, \delta\left(E_c(\varkappa) - E_v(\varkappa) - \hbar\,\omega\right). \qquad (8)$$

Let us now simplify the formula (7) by an assumtipon usually made in the theory of the optical properties of crystals, that $|\boldsymbol{p}_{v\,c}(k)|$ is a constant. We put

$$f(\varkappa, \varkappa') = N \left|\sum\limits_k {}_a\langle c\,\varkappa'|c\,k\rangle\,\langle v\,k|v\,\varkappa\rangle_a\right|^2, \qquad (9)$$

where $N = V/\Omega$ is the number of unit cells in the basic volume V. In a crystal $f(\varkappa, \varkappa') = N\,\delta_{\varkappa\varkappa'}$. As it is seen from (9), in an amorphous solid, $f(\varkappa, \varkappa')$ will have a finite maximum for $\varkappa = \varkappa'$ and a certain non-zero width. The double sum $\sum\limits_{\varkappa}\sum\limits_{\varkappa'} f(\varkappa, \varkappa')$ is independent of the actual form of $|v\,\varkappa\rangle_a$, $|c\,\varkappa'\rangle_a$ if these wave functions are constructed as described above and $|\boldsymbol{p}_{v\,c}|$ is a constant. In the crystal it gives

$$\sum\limits_{\varkappa}\sum\limits_{\varkappa'} f(\varkappa, \varkappa') = N \sum\limits_{\varkappa}\sum\limits_{\varkappa'} \delta_{\varkappa\varkappa'} = N \sum\limits_{\varkappa} 1 = N^2. \qquad (10)$$

Therefore, the following sum rule holds (Velický [23]):

$$\int\limits_B d^3\varkappa\, d^3\varkappa'\, f(\varkappa, \varkappa') = B^2. \qquad (11)$$

B is the volume in the reciprocal space of the Brillouin zone. The existence of a sum rule for $f(\varkappa, \varkappa')$ is expected from an intuitive reasoning. It replaces the δ-function by a function with a finite width which must obey the same normalisation equation.

With the function $f(\varkappa, \varkappa')$ (7) can be written

$$\varepsilon_2(\omega) = \left(\frac{2\pi e}{m\omega}\right)^2 \frac{2}{(2\pi)^3} \frac{1}{B} |\boldsymbol{p}_{v\,c}|^2 \int\limits_B d^3\varkappa\, d^3\varkappa'\, f(\varkappa, \varkappa')\, \delta\left(E_c(\varkappa') - E_v(\varkappa) - \hbar\,\omega\right). \quad (12)$$

We shall now discuss a particularly simple case that near $\varkappa = \varkappa' = 0$ the factor $f(\varkappa, \varkappa')$ is constant $(= f_0)$ in a certain part of the Brillouin zone B_0 and zero in the rest. From the sum rule (11) we determine f_0 to be B/B_0. In this case in the range considered (12) gives

$$\varepsilon_2(\omega) = \left(\frac{2\pi e}{m\omega}\right)^2 \frac{2}{(2\pi)^3} \frac{1}{B_0} |\boldsymbol{p}_{v\,c}|^2 \int d^3\varkappa\, d^3\varkappa'\, \delta\left(E_c(\varkappa') - E_v(\varkappa) - \hbar\,\omega\right) =$$

$$= \left(\frac{2\pi e}{m\omega}\right)^2 \frac{2}{(2\pi)^3} \frac{1}{B_0} |\boldsymbol{p}_{v\,c}|^2 \int dE \int d^3\varkappa'\, \delta\left(E_c(\varkappa') - E\right) \int d^3\varkappa\, \delta\left(E - E_v(\varkappa) - \hbar\,\omega\right) =$$

$$= \left(\frac{2\pi e}{m\omega}\right)^2 \frac{2}{(2\pi)^3} \frac{1}{B_0} |\boldsymbol{p}_{v\,c}|^2 \int dE\, g_c(E)\, g_v(\hbar\,\omega - E). \qquad (13)$$

It is apparent that $\varepsilon_2(\omega)$ is determined by a convolution of the densities of states in the valence and conduction bands $g_v(E)$ and $g_c(E)$ for which energy is conserved. If the energies are measured from the band extrema we have $g_v(E_p) \sim$ $\sim E_p^{1/2}$, $g_c(E_n) \sim E_n^{1/2}$, $E_n + E_p = \hbar\,\omega - E_g$. We obtain then from (13)

$$\omega^2\, \varepsilon_2(\omega) \sim (\hbar\,\omega - E_g)^2 \qquad (14)$$

in accord with observation.

The suggested approach allows a rough estimate of B_0 because $|\boldsymbol{p}_{v\,c}|$ and g_v, g_c are crystalline quantities and are known in Ge. We assume that the edge observed in amorphous germanium corresponds to $\Gamma_{2'} \to \Gamma_{25'}$ direct transition in the crystal. We calculate the densities of states with the effective masses $m_p = 0.49\,m$ (from the results in Section 4), $m_n = 0.04\,m$ (after [24]) and take $|\boldsymbol{p}_{v\,c}| = 7 \times 10^{-20}$ g cm s^{-1} (after [24]). The slope of the straight line in Fig. 4 is $d\hbar\omega\,\sqrt{\varepsilon_2}/d\hbar\omega = 6.5$. With these values we obtain from (13) $B_0 = 2.2 \times 10^{21}$ cm^{-3}; as $B = (2\pi)^3\,4/a^3 = 5.6 \times 10^{24}$ cm^{-3} we have $f_0 = 2.5 \times 10^3$. Therefore, the $\boldsymbol{k}$ vectors of the Bloch functions from which the wavefunctions of amorphous Ge are formed lie in a reciprocal volume of 0.04% of the reduced Brillouin zone.

According to the uncertainty relation, these combinations describe wave functions localised in real space in a volume $V_0 = (2\pi)^3/B_0 \approx 10^{-19}$ cm^3. This volume contains about 5000 atoms.

As the results discussed in Section 4 show that the wave functions of the valence bands are well described by Bloch functions, the localisation must be ascribed to the wave functions of the conduction band.

7. Conclusions

1. The absorption spectra observed in amorphous Ge in the spectral region 0.08 to 0.6 eV have a similar structure as in p-type doped crystals. They can be interpreted as direct transitions of holes between the three branches of the valence band. We obtain for the spin-orbit splitting $\Delta E = 0.20$ eV in non-annealed and $\Delta E = 0.21$ eV in annealed samples. The effective masses of holes are $m_1 = 0.49\,m$, $m_2 = 0.04\,m$, m_3 (the split-off band) $= 0.08\,m$ in non-annealed and $m_1 = 0.43\,m$, $m_2 = 0.04\,m$, and $m_3 = 0.08\,m$ in annealed samples. The concentration of holes is estimated to be about 10^{19} cm^{-3}.

2. The possibility of interpreting these spectra as $\boldsymbol{k}$ conserving transitions shows that the wave functions in the valence band near $\boldsymbol{k} = 0$ are not essentially different from those in the crystal.

3. In front of the intrinsic absorption edge there is a tail which cannot be explained as band to band or localized center to band transitions. It appeares unlikely that it is due to the distorted (more or less localized) states near the band edges which have been proposed by some theories of the electronic structure of amorphous solids. An important feature of the absorption in this tail is that it increases with increasing temperature. It is suggested that it may be due to excitons bound to neutral acceptors. These acceptors are probably the same defects (presumably vacancies) which have been shown to play a decisive role in the transport properties. For the excitation energy of these acceptors one has obtained $E_A \geqq 0.01$ eV.

4. Because of the presence of this tail, it is not possible to observe the perhaps present intrinsic tail due to the distortion of the bands states. Such a tail, if it actually exists, may be observable at sufficiently low temperatures.

5. The absorption at the edge is described by the relation $\omega^2\,\varepsilon_2 \sim (\hbar\omega - E_g)^2$ which is interpreted as due to indirect transitions.

It is shown that this result can be understood if the wave functions in the bands are linear combinations of the Bloch functions of the same band in the crystal. Taking the densities of states to be the same as in the crystal and making some assumptions on the matrix elements it is found that the linear combinations extend over $\boldsymbol{k}$ vectors from about 0.04% of the reduced Brillouin zone of crys-

talline Ge. This means a localization of the wave functions in a volume of about 10^{-19} cm^3 containing about 5000 atoms.

6. As the valence band wave-functions appear to be well described by Bloch functions (cf. point 2), the localization must be ascribed to the conduction band wave-functions. It appears that a different degree of localization belongs to various parts of the band structure.

The paper on the optical properties in the main absorption band and valence band plasma region is in preparation.

Acknowledgements

References

[1] J. L. HARTKE and P. J. REGENSBURGER, Phys. Rev. **139**, A 970 (1965).

[2] H. RICHTER and G. BREITLING, Z. Naturf. **13a**, 988 (1958).

[3] J. D. MACKENZIE, Modern Aspects of the Vitreous State, Vol. I, Butterworth, London 1960.

[4] R. GRIGOROVICI, N. CROITORU, A. DÉVÉNYI, and E. TELEMAN, 7th Conf. Physics of Semiconductors, Paris 1964 (Dunod, Paris 1964) (p. 423).

[5] M. P. LISITZA and N. G. TSVELICH, Optika i Spektroskopiya **5**, 622 (1958).

[6] J. TAUC, A. ABRAHÁM, L. PAJASOVÁ, R. GRIGOROVICI, and A. VANCU, Proc. Internat. Conf. Physics of Noncrystalline Solids, Delft 1964. North Holland Publ. Comp. 1965 (p. 606).

[7] R. SUHRMANN, M. KRUEL, and G. WEDLER, Z. Phys. **173**, 71 (1963).

[8] A. VAŠKO, Infračervené záření a jeho užití, Státní nakladatelství technické literatury, Praha 1963 (p. 155) (in Čzech.).

[9] A. ABRAHÁM, Československý časopis pro fysiku **A14**, 24 (1964) (in Čzech.).

[10] F. LUKEŠ, Czech. J. Phys. **9**, 118 (1959).

[11] H. MAYER, Physik dünner Schichten I, Wissensch. Verlagsgesellschaft, Stuttgart 1950 (p. 168).

[12] K. KOLLER, Z. Phys. **110**, 661 (1938).

[13] H. B. BRIGGS and R. C. FLETCHER, Phys. Rev. **87**, 1130 (1952); **91**, 1342 (1953).

[14] W. KAISER, R. COLLINS, and H. Y. FAN, Phys. Rev. **91**, 1380 (1953).

[15] R. NEWMAN and W. W. TYLER, Phys. Rev. **105**, 885 (1957).

[16] A. H. KAHN, Phys. Rev. **97**, 1647 (1955).

[17] E. O. KANE, J. Phys. Chem. Solids **1**, 82 (1956).

[18] F. R. KESSLER and E. SUTTER, Z. Phys. **173**, 54 (1963).

[19] H. M. JAMES and K. LARK-HOROWITZ, Z. phys. Chem. **198**, 107 (1951).

[20] F. SEITZ, Rev. mod. Phys. **26**, 7 (1954).

[21] A. I. GUBANOV, Quantum Electron Theory of Amorphous Conductors, Consultant Bureau, New York 1965 (in Russian, Izd. Akad. Nauk, Moskva 1963).

[22] K. MOORJAMI and C. FELDMAN, Rev. mod. Phys. **36**, 1042 (1964).

[23] B. VELICKÝ, to be published.

[24] M. CARDONA, J. Phys. Chem. Solids **24**, 1543 (1963).